

Rapid and automatic evaluation of the performance of phosphor screens for image intensifiers

RONGSHENG ZHU, BO YANG, MING JI, JIE XIAO, ZHIXIONG SHI, ZENGWEI LI, LISONG ZHANG, HANG ZHAO, TIANNING SU, FENGGE LIU*

Department of Operation Support, North Night Vision Technology Co. Ltd., 650217, Kunming, China

Improvement of the detection accuracy and efficiency of phosphor screen performance for the image intensifier is not only a requirement for objectively evaluating the performance of the phosphor screen, but also a key step in enhancing product quality. A powerful way to address this problem is to achieve rapid and automatic evaluation of phosphor screen performance for image intensifiers. Key challenges that need to be overcome include automatic operation of the vacuum system and the servo system, and the design of large-area uniform electron sources. To achieve this goal, we have taken some strategies. Through reasonable design of vacuum control, the automatic adjustment and maintenance of vacuum levels can be achieved. The automatic operation of servo system has been accomplished by precisely controlling the speed and direction of the servo motor. Good luminance uniformity of phosphor screen can be ensured by designing a uniform planar electron source with a diameter of 50 mm. In conjunction with matching our software, a rapid and automatic measurement system of the phosphor screen performance for image intensifiers has been developed. To validate the performance of this system, we selected 300 phosphor screens for low-light-level image intensifiers with a diameter of 18 mm as measurement samples, grouping them into sets of 30. Subsequently, we measured their luminance, luminous efficiency, uniformity and defect, thereby obtaining the repeatability error and detection efficiency of measurement system. The experimental results show that the measurement data of luminance, luminous efficiency, uniformity and defect meet practical requirements well. The repeatability errors for luminous efficiency and uniformity are 3.036% and 0.369%, respectively, which conform to the measurement standards. More importantly, the detection accuracy of defect reaches 93.45%, and the detection time for a single phosphor screen is only 18.2s, which is much shorter than 52.6s required for manual inspection. Therefore, this measurement system has perfectly achieved rapid and automatic evaluation of the performance of 30 phosphor screens with a diameter of 18 mm each time, providing an objective evaluation method to improve the performance of phosphor screen for image intensifiers.

(Received October 19, 2024; accepted February 3, 2025)

Keywords: Automatic evaluation, Phosphor screen, Luminance, Luminous efficiency, Uniformity, Defect

1. Introduction

Image intensifiers are electron-optical devices that are used to detect and intensify optical images in the near ultraviolet, visible, near infrared, X-ray and gamma-ray regions. Accordingly, they are used for night vision, astronomy, X-ray and gamma-ray intensification etc. [1-3]. In general, a commercial proximity-focused image intensifier consists of a photocathode for the conversion of the incident radiant image to a low-energy electron image, of microchannel plate (MCP) for electron multiplication, and of a phosphor screen for converting a high-energy electron image into an intensified light image. Since the basic function of the phosphor screen is to convert the electron beam energy into light, logically, the performance of this phosphor screen has a significant impact on image quality of the image intensifier, and then this fact has been validated [4-6]. The key performance indicators of a phosphor screen for the image intensifier mainly include luminous efficiency, luminance, luminance uniformity and defect distribution. In practice, it is necessary to implement accurate evaluation of the above indicators for enhancing the performance of phosphor screen and thus improving the image quality of image intensifiers [7].

In terms of the performance evaluation of phosphor screen for image intensifiers, extensive work on the luminous efficiency evaluation of phosphor powder, the lifetime evaluation and the afterglow evaluation of phosphor screen has been reported in the literature [8-13]. Additionally, most research into performance evaluation of image intensifier has focused on resolution, photocathode diameter, and structural defects of low-light-level (LLL) image intensifier, however, detailed studies on performance evaluation of phosphor screen have not been received much attention [14-19]. More importantly, existing but limited evaluation methods of phosphor screen performance for image intensifiers have mostly utilized manual visual inspection, which leads to a relatively low accuracy and reliability [20, 21]. Hence, these limitations are insufficient to meet the requirements of fabrication and yield rate of commercial phosphor screen for image intensifiers. An extremely effective solution is to optimize the fabrication process of phosphor screen, and that is obtained by rapid and automatic evaluation of phosphor screen performance.

To achieve rapid and automatic evaluation of phosphor screen performance for image intensifiers, it is essential to develop a matching automatic measurement system. Specifically, main challenges in developing this system are

how to achieve automatic control of high vacuum automatic switching of test station and achieve rapid automatic measurement of luminance, luminous efficiency, uniformity, and defect distribution. It is the purpose of this paper to overcome these challenges by designing vacuum system, servo system, uniform planar electron source, image acquisition system, and appropriate software. Eventually, the rapid and automatic evaluation of multi-station batch of phosphor screen for image intensifiers will be implemented.

2. Measurement principle

2.1. Measurement principle of luminance

Luminance of phosphor screen is defined as the luminous flux radiated from light source within per unit area and per unit solid angle in the direction perpendicular to the surface of phosphor screen, measured in cd/m^2 . It is numerically equal to the luminous intensity per unit projected area, as shown in Fig. 1. Here, ds denotes luminous surface, I_θ is luminous intensity, L represents luminance. Obviously, the values of luminance are not the same in different directions.

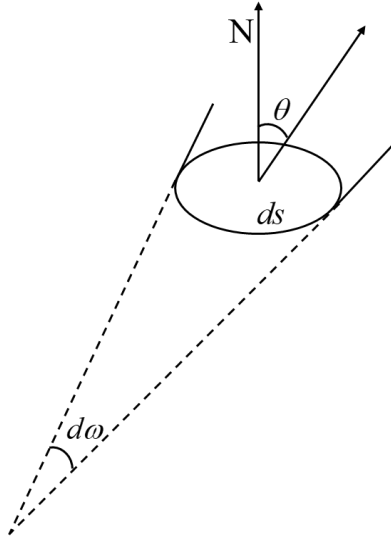


Fig. 1. Schematic diagram of luminance per unit area

If luminous surface ds is an ideal diffuse reflector and luminous intensity I_θ obeys the cosine law, the luminance L is independent of direction, it can be stated as follows

$$L = \frac{I_\theta}{ds} \quad (1)$$

With regard to phosphor screen for image intensifiers, it can be considered as ideal diffuse reflector and corresponding luminous intensity complies with approximately cosine distribution. Therefore, luminance of

phosphor screen can be obtained by calculating the average grayscale of image acquired by high-resolution camera.

2.2. Measurement principle of luminous efficiency

The luminous efficiency of a phosphor screen refers to its ability to convert the input energy into visible light after being bombarded by electrons. It is defined as the luminescence intensity generated by the energy of electron beam bombarding phosphor screen. In practice, luminous efficiency is typically expressed in terms of lumen efficiency, namely, the ratio of luminous flux radiated from phosphor screen to power of exciting electron beam, measured in lm/W . Concretely, it is given by

$$\eta = \frac{\phi}{P} = \frac{\phi}{UI} = \frac{\phi}{UjS} \quad (2)$$

where η is luminous efficiency (lm/W), ϕ is luminous flux radiated from phosphor screen (lm), P denotes power of exciting electron beam (W), U is phosphor screen voltage (V), I is current of electron beam (A), S is area of phosphor screen (m^2), and j represents density of exciting electron beam (A/m^2), respectively.

According to the above definition of luminance of phosphor screen, clearly, ϕ is described by luminance and then takes the form of

$$\phi = SR = 2\pi SL \quad (3)$$

where R is luminance per unit area (lm/m^2). Combining formula (1) and (2), luminous efficiency of phosphor screen η can be obtained by

$$\eta = \frac{2\pi L}{Uj} \quad (4)$$

in other words, we can determine the value of luminous efficiency.

2.3. Measurement principle of uniformity

The uniformity of phosphor screen for image intensifiers is one of the key performance indicator that directly affects imaging quality. According to national military standard GJB2000A-2020 general specification for image intensifiers, the value of uniformity should be less than or equal to 3. This means that luminance distribution within the luminous area of phosphor screen must be sufficiently uniform and with no abrupt or noticeable boundaries between bright and dark. Currently, measurement methods of luminous uniformity of phosphor screen mainly include narrow-sense non-uniformity method, fixed pattern noise method, and image grayscale method. It is important that the first two methods are based

on overall performance of the image intensifier and then to process and analyse the image of phosphor screen. If any indicator of components, such as fiber optic panel, electron optical system, photocathode, and phosphor screen, does not satisfy the requirements, it may lead to non-uniform luminance of the image. Therefore, we use image grayscale measurement method to evaluate luminance uniformity of phosphor screen for image intensifiers. Measurement principle of image grayscale method is described as follows.

Using a high-resolution camera, the luminous image of phosphor screen is converted into a digital image. By analysing this digital image, the given luminous area of phosphor screen has been marked. Subsequently, the maximum and minimum grayscale values within a specified area are extracted based on luminance characterised by grayscale values. These values represent the range of luminance variation within the given area. Ultimately, the ratio of the maximum value to the minimum value would determine the luminance uniformity, which is used to evaluate whether the phosphor screen meets GJB2000A-2020 general specification.

2.4. Detection principle of defect

According to the definition in national military standards, defects on phosphor screen are regarded as bright spots, opaque spots, and dark spots exceeding the specified contrast on the phosphor screen, which directly affect the image quality of image intensifiers. Moreover, in terms of U.S. military specifications for night vision devices, any spot with a luminance difference of 30% or more compared to surrounding background is considered as a defect. It should be emphasized that, for different types of phosphor screens such as P22, P43, P46, and P47, the size and quantity of defects must meet specific technical requirements. As a result, we must present an objective detection method of defects on phosphor screen for image intensifiers.

The detection method of defects on a phosphor screen for image intensifiers is given as follows. Firstly, by adjusting the brightness of the phosphor screen to an optimal level, the best contrast for identifying defects can be obtained. Secondly, through adjusting the microscope magnification, a ratio of 1:1 between the image and actual object is achieved. Thirdly, using a high-resolution camera, the illuminated image from phosphor screen is converted into a digital image. More importantly, in order to identify defects, edge detection is used to determine the position and boundaries of luminance area. Then, the circular extraction of luminance region can be done. Using the multi-threshold maximum-class variance method, the luminous regions of phosphor screen are segmented into different sections. It determines threshold values for different luminous regions and forms a set of thresholds that maximizes inter-class variance while minimizes intra-class variance. To perform

connected component analysis on thresholded images, we apply eight-neighbourhood criteria to mark the connected regions. Simultaneously, the area properties of each marked region are recorded by counting the total number of target pixels in that connected component. Afterwards, all marked images must be traversed, and if the marked value at a given region is i , the area S_i of the i -th connected component is incremented by 1. Continue this process until that the entire image has been traversed, the expression of S_i is given by

$$S_i = \sum_{x=1}^m \sum_{y=1}^n (p(x, y) = i) \quad (5)$$

Lastly, by sorting the connected areas in ascending order and retaining only those regions with areas larger than a definite threshold, all defects with a brightness difference of 30% compared to surrounding background can be identified.

3. Rapid and automatic measurement system

From a production point of view, dozens of phosphor screen need to be measured in batches. However, traditional manual inspection methods cannot guarantee the consistency of testing standards. In addition, human eyes are unable to cope with high-intensity testing, leading to a decrease in work efficiency. To address this problem, we have developed a rapid and automatic measurement system of phosphor screen performance for image intensifiers, based on above measurement principle. This automatic measurement system aims to enhance the consistency of batch testing standards and to improve work efficiency via replacing manual visual inspection with machine automation. Particularly, this system enables rapid and automatic detection of luminance, luminous efficiency, uniformity, and defect of phosphor screen.

3.1. General description

As shown in Figs. 2a and 2b, the measurement platform consists of a vacuum system, servo control system, uniform planar electron source, high-voltage control system, and image acquisition system. More concretely, in Fig. 2a, 1 is test station, 2 is high valve, 3 is observation window, 4 is top cover, 5 is vacuum chamber, 6 is planar electron source, and 7 is transmission device. In Fig. 2b, 8 is camera and microscope mount, 9 is vent valve, 10 denotes electric cylinder and servo motor, 11 represents high-voltage input terminal, 12 is vacuum gauge, 13 is loading cabinet, and 14 is operating platform, respectively.

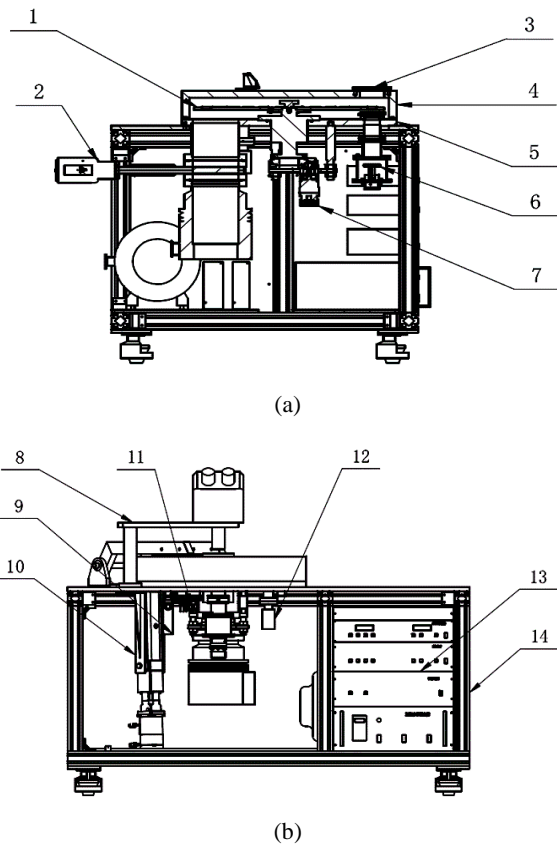


Fig. 2. (a) Side view diagram of automatic measurement system; (b) Front view diagram of automatic measurement system

The vacuum system achieves a vacuum level of 2×10^{-3} Pa within 30 minutes that is essential environment for measurement. The role of servo control system is not only to enable rapid and stable switching between 30 stations with a diameter of 18 mm each and 24 stations with a diameter of 24 mm each, but also to automate the reset of measurement stations. The uniform planar electron source provides a large-area uniform electron surface and ensures uniform illumination of the phosphor screen. The high-voltage control system is responsible for applying suitable voltage to both the planar electron source and the phosphor screen, which enables electron emission and screen illumination. The main task of the image acquisition system is to capture images from phosphor screen and then to analysis corresponding image data. In the end, rapid and automatic evaluation of luminous efficiency, luminance, uniformity, and defects can be conducted. Fig. 3 shows physical setup of rapid and automatic measurement system of phosphor screen performance for image intensifiers. The following section focuses on the designs of vacuum system, servo control system, uniform planar electron source, and corresponding software.



Fig. 3. Picture of rapid and automatic measurement system of phosphor screen performance for image intensifiers

3.2. Design of vacuum system

To obtain the vacuum level of 2×10^{-3} Pa within 30 minutes, we have designed a vacuum system and corresponding structural schematic diagram has been given in Fig. 4. This vacuum system mainly consists of a vacuum controller, top cover, vacuum chamber, vacuum gauge, a mechanical pump, and a molecular pump. Additionally, it includes various valves controlling airflow, such as low-pressure valve, front stage valve, high-pressure valve, and vent valve.

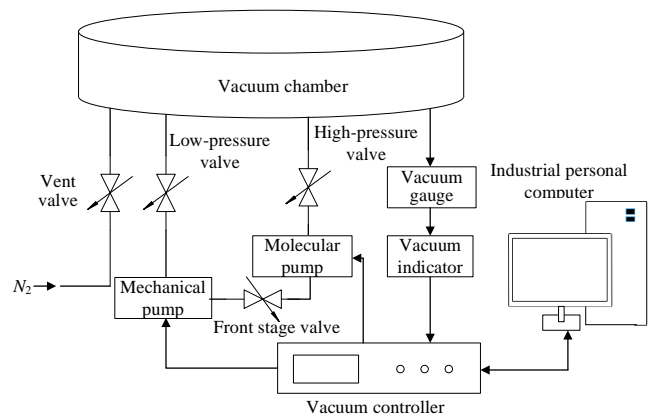


Fig. 4. Structural schematic diagram of vacuum system

In order to enable the automatic operation of vacuum system and to facilitate troubleshooting and maintenance, we have designed a system control logic tailored to the vacuum controller. In addition, it is compatible with both automatic and manual operation modes. The functions of this control logic are divided into two parts: the first is the vacuum control that is responsible for adjusting and maintaining vacuum level required for testing; the second is

the sample replacement control that ensures these samples can be changed quickly.

Upon activating the vacuum extraction command, vacuum controller first performs a comprehensive status check on hardware components involved in the system. The primary focus is on vacuum valves, specifically, if any valve is found to be in an unexpected open state, it immediately triggers a closing action. This ensures the integrity of the chamber's seal and overall safety of the vacuum system. When all valves are confirmed to be closed, the pre-pumping process for the vacuum chamber by opening the mechanical pump and low-pressure valve. In the meanwhile, the vacuum gauge continuously monitors the vacuum level of the chamber in real-time. Once the vacuum level reaches the threshold of 10 Pa, vacuum controller closes promptly the low-pressure valve. Whereafter, the system activates front stage valve and molecular pump. When the molecular pump reaches a rotational speed of 70 r/s, the high-pressure valve is opened. Note that the rotational speed of molecular pump will continue to increase until it reaches the rated speed of 820 r/s. As a result, the vacuum level inside the chamber will rapidly decrease until that the desired operating vacuum level of 2×10^{-3} Pa is achieved.

As for stopping the vacuum extraction, vacuum controller will close all valves except for front stage valve, and then verify whether all other valves are indeed closed. Once it is confirmed, shutdown of the molecular pump has been done. When the rotational speed of molecular pump drops to 70 r/s, front stage valve and mechanical pump are automatically closed. So far, the full shutdown of vacuum system is completed. By turn, as the sample replacement command is activated, vacuum controller immediately initiates the closure of all valves except for front stage valve. After ensuring valve states meet the given conditions, vacuum controller maintains molecular and mechanical pump at full operational speed. During this process, by opening the vent valve, nitrogen is slowly injected into vacuum chamber. This helps to prevent potential moisture or contaminants from affecting the vacuum system or samples.

When the vacuum level reaches the designated 1×10^5 Pa, vacuum controller sends an enable signal to the upper computer, and then confirms that the sample replacement is ready. Upon receiving the enable signal, the upper computer controls top cover to lift, allowing the testing personnel to confirm that the replacement of phosphor screen is complete. Since the sample replacement is complete, vacuum system can proceed with the vacuum extraction. By the above means, the dual-mode operation function of vacuum controller can be implemented. Testing personnel can opt for fully automatic mode, enabling the vacuum system to operate automatically.

3.3. Design of servo control system

In a bid to accommodate the measurement of phosphor screen with diameter of 18 mm and 24 mm, we have designed a testing turntable with 30 stations for the

diameter of 18 mm and a turntable with 24 stations for the diameter of 24 mm. To enable automatic station switching and turntable resetting, a servo control system has been designed and illustrated in Fig. 5. Specifically, 1 is turntable lock pin, 2 is phosphor screen testing turntable, 3 is transmission device, 4 is industrial sensor, and 5 is servo drive component, respectively. The servo drive component consists of a servo motor offering output power of 400 W and a servo driver of Panasonic MBDLT25SF model. By controlling the servo drive component, the transmission device can be rotated, enabling the switching of test stations. Additionally, the control signal of the industrial sensor is responsible for resetting the testing turntable.

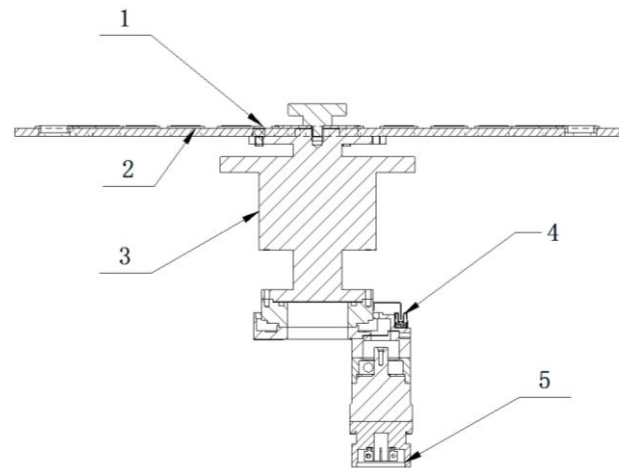


Fig. 5. Structural schematic diagram of servo control system

For the automatic operation of this servo control system, it is very important to implement remote control of servo system via an upper computer based on MODBUS communication protocol. The upper computer sends commands to the servo driver via RS232, and this driver automatically calculates the number of pulses required for switching stations. And then it enables precise control over the speed and direction of servo motor, naturally, smooth switching between any stations on the testing turntable can be obtained. In addition, the servo control system incorporates an automatic reset function, and thus test turntable will accurately return to the absolute zero position at the end of each measurement cycle. This provides a reference zero point for next round of measurement. Namely, the servo control system can effectively reset and resume accurate work cycles when this system starts up or stops with an unexpected shutdown. Consequently, automatic operation of the servo control system can be achieved.

3.4. Design of uniform planar electron source

The filament of electron gun is wound into a circular shape, and it has been used in measurement system of phosphor screen performance. However, the diameter of the multiplied electron beam does not completely match the

diameter of phosphor screen, resulting in measurement errors. To address the limitation of thermionic emission guns, which rely on filaments for thermionic emission and can only provide a small-area uniform electron beam, a large-area (diameter of 50 mm) uniform planar electron source has been designed. It consists of a UV lamp, a photolithography steel mesh, a gold cathode, and a microchannel plate (MCP).

The disk-shaped UV lamp serves as the emission light source, emitting uniform ultraviolet light externally. A photolithography steel mesh with a diameter of 106 mm and 50 holes can ensure the intensity and uniformity of emitted light distribution. The energy of excitation light is converted into photoelectrons by a gold cathode, and the output electron flow is multiplied by the MCP with diameter of 50 mm. The operational workflow of large-area uniform planar electron source is as follows: the UV lamp

provides a high-intensity ultraviolet light source, and it passes through the photolithography mesh, which causes the gold cathode to emit a large number of electrons. These electrons are then multiplied by MCP, resulting in a large-area uniform electron emission.

3.5. Development of matching software

In order to achieve rapid and automatic evaluation of phosphor screen performance for image intensifiers, we have specifically developed matching software. The software is designed on Visual Studio 2013 platform and is developed by C++ language in conjunction with Microsoft Foundation Class (MFC) library. As shown in Fig. 6, it is divided into four functional modules: initialization module, joint-control module, image acquisition module, and automatic test module.

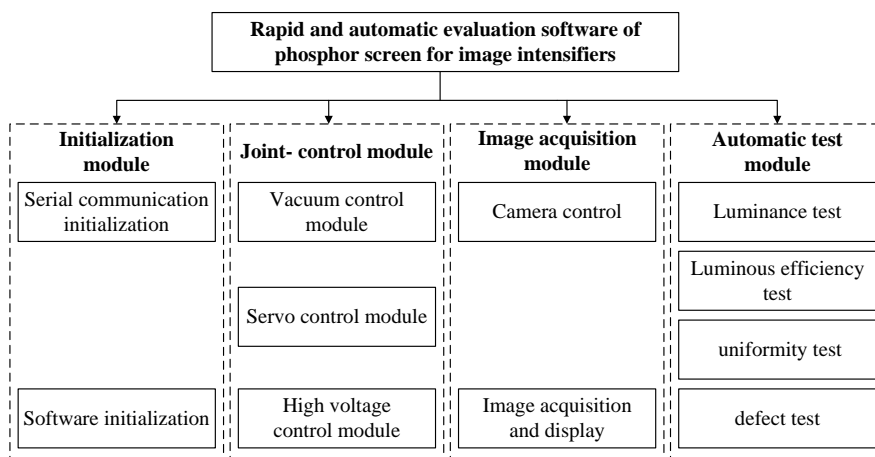


Fig. 6. Structural schematic diagram of software

The initialization module aims to set up the serial port and software parameters. By reading the serial port parameter values set in the program, the connection with each hardware device is made. To enable remote control and automatic operation of the servo drive components, vacuum controller, high-voltage control, and uniform planar electron source, it is necessary to design an instrument joint-control module. This joint-control module consists of three sub-modules: vacuum control module, servo control module, and high-voltage control module.

The vacuum control module can provide a stable testing environment by achieving synchronized control of multiple vacuum devices and synchronized data transmission from each device. What is remarkable is that this vacuum control module enables one-click operation for turning vacuum system on and off, one-click replacement of sample, and one-click control of top cover, vent valve, and UV lamp. At the same time, it also provides real-time display of vacuum level. The servo control module enables one-click switching of station, automatic reset of test turntable, and switching between 30 phosphor screens with diameter of 18 mm or 24 phosphor screen with diameter of 24 mm. The high-voltage control module is designed to

allow for flexible adjustment of the operating voltage for both uniform planar electron source and phosphor screen.

The image acquisition module primarily includes functions of camera activation and deactivation, exposure time settings, image save settings, and real-time display of image. By activating the camera, the acquisition module automatically initializes exposure time and grayscale dynamic range of the camera. Subsequently, the acquired image is real-time displayed on the image display interface. Moreover, we can obtain display frame rate, acquisition frame rate, and the average grayscale dynamic range of current image. The parameter automatic testing module is designed to perform fully automatic comprehensive testing of luminance, luminous efficiency, uniformity, and defect identification of phosphor screen for image intensifiers. Fig. 7 shows the software interface for automatic batch testing system of phosphor screen performance for image intensifiers.

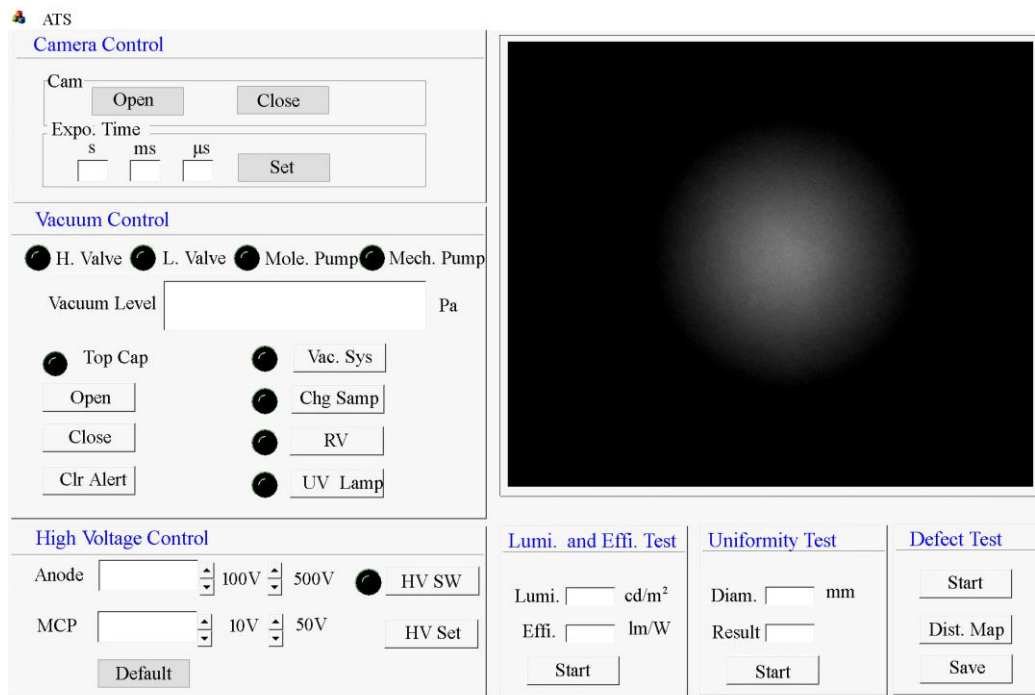


Fig. 7. Software interface for automatic measurement system of phosphor screen performance

4. Results and discussions

4.1. Verification of vacuum level

According to actual measurement requirements, the vacuum level must to reach an absolute operational value of 2×10^{-3} Pa within 30 minutes at room temperature. Whereas, for the sake of improving performance measurement efficiency of commercial phosphor screens, it is necessary to achieve a relative operational vacuum level of 5×10^{-3} Pa within 15 minutes at room temperature. Once this relative vacuum level is reached, the performance measurement of phosphor screen should begin promptly.

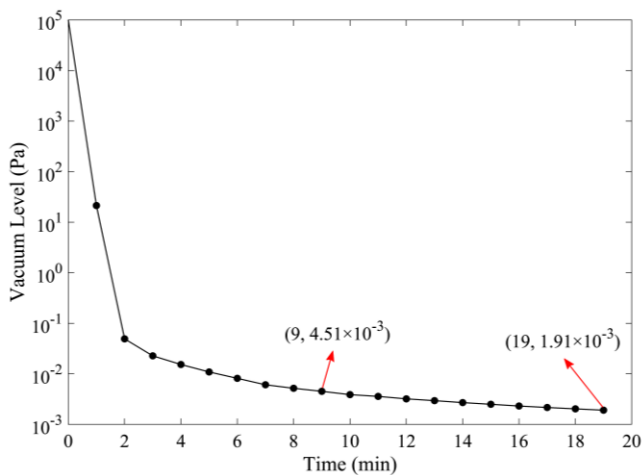


Fig. 8. Curve of vacuum level versus time

When the automatic measurement system of phosphor screen is in full-load operation at room temperature, vacuum extraction performance is tested. It is done by conducting five sets of tests daily over a continuous period of 10 days. One group of test data is randomly selected, resulting in the relationship between vacuum level versus time data, as shown in Fig. 8.

As can be seen from Fig. 8, the relative operational vacuum level within chamber reaches 5×10^{-3} Pa within 9 minutes, and the absolute operational vacuum level reaches 2×10^{-3} Pa within 19 minutes. Obviously, this vacuum system is sufficient to meet actual measurement requirements of phosphor screen performance for image intensifiers.

4.2. Measurement of luminance

The luminance of a phosphor screen is not only a crucial indicator of its quality but also significantly affects its performance in various application. In the case of a phosphor screen for the image intensifier, the luminance directly affects the clarity and discernibility of the image. Accordingly, the optimization of luminance of phosphor screens is an essential objective in their design and fabrication. Apart from the phosphor material, the energy and intensity of electron beam are key factors affecting the luminance of phosphor screen. The former can be represented by the voltage of phosphor screen, and the latter is denoted by the current of phosphor screen. Naturally, it is important to reveal the dependence of luminance on voltage and current of phosphor screen through measurement data.

4.2.1. Effect of current on luminance

To establish a model of the relationship between the luminance and current of phosphor screen, we have set the experimental conditions and taken experimental steps as follows. The samples of phosphor screen with diameter of 18 mm for widely-used LLL image intensifiers have been selected to be measured. Note that samples of the same model will be chosen for the following experiments. Under the circumstances of fixing the voltage of phosphor screen at 6000 V, we have varied MCP voltage starting at 600 V and increased by steps of 20 V until 800 V. The variation of the current of phosphor screen has been achieved by adjusting the voltage across MCP. Thereupon, the luminance of 150 phosphor screen samples have been measured, and a group of experimental data has been randomly selected for analysis. Table 1 shows these experimental data.

Table 1. Data of luminance and current of phosphor screens

Order	Voltage across MCP (V)	Current of phosphor screen (μA)	Luminance (cd/m^2)
1	600	0.16	2.44
2	620	0.21	3.67
3	640	0.27	4.79
4	660	0.33	6.07
5	680	0.41	7.63
6	700	0.52	9.53
7	720	0.63	11.83
8	740	0.77	14.57
9	760	0.93	17.71
10	780	1.12	21.14
11	800	1.37	24.68

From Table 1, it is clear that the luminance of phosphor screen increases with increasing the current of phosphor screen, and they exhibit an approximately linear relationship. Furthermore, by establishing a linear regression model, the resulting relationship between luminance (L) and current (I) is given by

$$L = 18.77I - 0.175 \quad (6)$$

Besides, by performing a R-value analysis on this model, the fitted curve is illustrated in Fig. 9. Apparently, the relationship between the luminance of phosphor screen and the current of phosphor screen is linear when the voltage across MCP ranges from 600 V to 800 V.

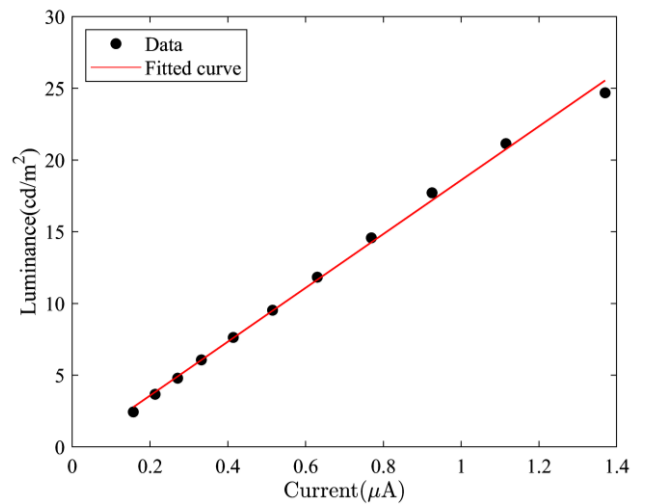


Fig. 9. Fitted curve of relationship between luminance and current

4.2.2. Effect of voltage on luminance

According to measurement results of luminance of phosphor screen and current of phosphor screen, the maximum value of luminance is obtained when the current is 1.37 μA . Therefore, to clarify the effect of voltage on luminance, the following measurement conditions must be determined. The current of phosphor screen is fixed at 1.37 μA , and the voltage of phosphor screen is starting from 2000 V and increasing in increments of 400 V, up to a maximum of 6000 V. The corresponding measurement results are shown in Table 2.

Table 2. Data of luminance and voltage of phosphor screens

Order	Voltage of phosphor screen (V)	Luminance (cd/m^2)
1	2000	0.023
2	2400	2.02
3	2800	4.58
4	3200	6.66
5	3600	9.01
6	4000	11.39
7	4400	14.83
8	4800	16.49
9	5200	19.02
10	5600	22.48
11	6000	24.68

Table 2 shows that the luminance of phosphor screen increases with increasing the voltage of phosphor screen, and they reveal an approximately linear relationship as well. Concretely, the relationship between luminance L and

voltage U is clarified by establishing a linear regression model expressed as equation (7).

$$L = 0.0062U - 13.0114 \quad (7)$$

Then, the fitted curve is illustrated in Fig. 10. Obviously, the relationship between the luminance and voltage of phosphor screen is linear.

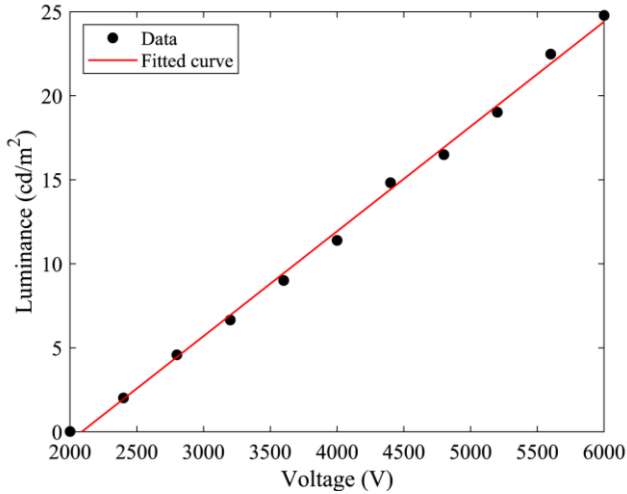


Fig. 10. Fitted curve of relationship between luminance and voltage

The above discussion have demonstrated that the correlation between the luminance of phosphor screen and current or voltage. Under the condition of a fixed current, the luminance exhibits a linear relationship with voltage. Similarly, when the voltage keeps a suitable constant, the luminance varies linearly with the current. In conclusion, within a certain range, the luminance of phosphor screen exhibits predictability under single-variable control. More importantly, the quantitative predictions of luminance based on equations (6) and (7) can provide a theoretical guide for achieving optimal luminance of phosphor screen used in general image intensifiers.

4.3. Measurement of luminous efficiency

Luminous efficiency is commonly used to evaluate the performance of phosphor screen materials and their suitability for specific applications. In image intensifiers, the improvement of the luminous efficiency of phosphor screen can enhance the overall performance and image quality of the device. Since luminous efficiency is mainly governed by the type of phosphor material, the energy and intensity of electron beam, it is significant to discuss the dependence of luminous efficiency on voltage and current of the phosphor screen.

4.3.1. Effect of current on luminous efficiency

To elucidate the effect of current on luminous efficiency of phosphor screen, we have set the experimental conditions and taken experimental steps as follows. On condition that the voltage of phosphor screen is fixed at 6000 V, we have varied MCP voltage increased by steps of 20 V from 600 V up to 800 V. Next step: the luminance of 150 samples of phosphor screen have been measured, and a group of experimental data has been randomly selected for analysis. Corresponding experimental data is shown in Table 3.

Table 3. Data of luminous efficiency and current of phosphor screens

Order	Voltage across MCP (V)	Current of phosphor screen (μA)	Luminous efficiency (lm/W)
1	600	0.16	4.32
2	620	0.21	4.63
3	640	0.27	4.86
4	660	0.33	4.95
5	680	0.41	5.12
6	700	0.52	5.22
7	720	0.63	5.28
8	740	0.77	5.25
9	760	0.93	5.30
10	780	1.12	4.99
11	800	1.37	4.84

From Table 3, it can be seen that the luminous efficiency of phosphor screen initially increases and then decreases as the current of phosphor screen increases. Additionally, the value of luminous efficiency reaches its maximum when the current is 0.93 μA . With a polynomial regression analysis between luminous efficiency and current of phosphor screen, the model has been established and is in the form of

$$\eta = 2.0028I^3 - 6.4565I^2 + 5.0097I + 3.5982 \quad (8)$$

Accordingly, the fitted curve is plotted in Fig. 11. There is a significant positive correlation between the luminous efficiency of phosphor screen and the current. However, this relationship exhibits nonlinearity.

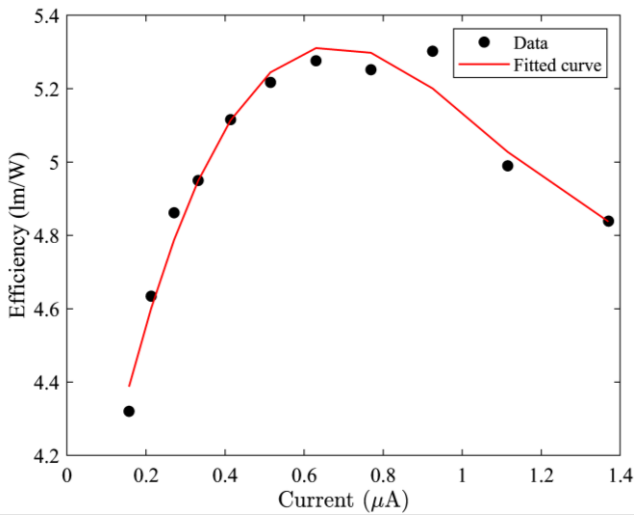


Fig. 11. Fitted curve of relationship between luminous efficiency and current

4.3.2. Effect of voltage on luminous efficiency

In the light of measurement data of luminous efficiency and current of phosphor screen, luminous efficiency reaches the maximum value when the current value is 0.93 μA. Nevertheless, the luminance does not reach its maximum value at this moment. In fact, measurement must be implemented with the premise that the luminance of phosphor screen need to reach its maximum value. Therefore, the current of phosphor screen is fixed at 1.37 μA, while the voltage of phosphor screen is changed in increments of 400 V from 2000 V to 6000 V. The measurement result has been shown in Table 4.

Table 4. Data of luminous efficiency and voltage of phosphor screens

Order	Voltage of phosphor screen (V)	Luminous efficiency (lm/W)
1	2000	0.01
2	2400	0.13
3	2800	0.44
4	3200	0.95
5	3600	1.59
6	4000	2.20
7	4400	2.83
8	4800	3.42
9	5200	3.94
10	5600	4.41
11	6000	4.82

Table 4 shows that the luminous efficiency of phosphor screen exhibits an incremental trend with increasing voltage, and the luminous efficiency reaches the maximum

value at a voltage of 6000 V. A polynomial regression analysis of luminous efficiency versus current of phosphor screen has been conducted, resulting in the model expressed by equation (9).

$$\eta = -9.876 \times 10^{-11} U^3 + 1.238 \times 10^{-6} U^2 - 0.004U + 2.955 \quad (9)$$

Simultaneously, the fitted curve is plotted in Fig. 12.

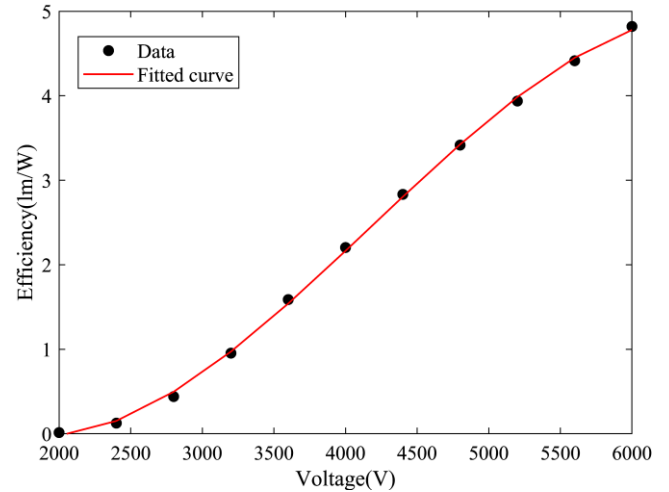


Fig. 12. Fitted curve of relationship between luminous efficiency and voltage

In summary, the above quantitative analysis reveals the interrelationship between luminous efficiency and current, and voltage. These experimental data demonstrate that, with a fixed current of phosphor screen, the relationship between luminous efficiency and voltage is nonlinear. Similarly, the luminous efficiency varies nonlinearly with the current when the voltage is constant. Furthermore, the luminous efficiency is predictable within a certain range and under single-variable (current or voltage) control. It should be emphasized that both models in equations (8) and (9) have successfully predicted the luminous efficiency of phosphor screen within a given range of current and voltage, which can provide theoretical guide for improving the luminous efficiency.

4.4. Measurement of uniformity

The significance of accurate measurement results of luminance uniformity of phosphor screens can not only ensure clarity and detail in displayed images, but also help manufactures identify problems in the production process, optimize material selection and techniques, and improve product quality. In addition, appropriate accelerating voltage and electron beam current can enhance the response speed and luminance of the phosphor screen, allowing it to maintain uniformity under different conditions. Therefore, we will measure uniformity of phosphor screen samples

and verify the performance of automatic measurement system of phosphor screen for the image intensifier.

4.4.1. Uniformity at different currents

For the case when the voltage of phosphor screen is fixed at 6000 V, we have varied MCP voltage increased by steps of 20 V from 700 V up to 800 V. The measurement results of uniformity and current of phosphor screens are illustrated in Table 5.

Table 5. Data of uniformity and current of phosphor screens

Order	Voltage across MCP (V)	Current of phosphor screen (μA)	Uniformity
1	700	0.52	1.58
2	720	0.63	1.61
3	740	0.77	1.63
4	760	0.93	1.67
5	780	1.12	1.74
6	800	1.37	1.81

As can be seen from Table 5, it is the fact that the luminance uniformity of phosphor screen shows little variation as the current increases within a certain range. More importantly, the values of uniformity are all less than 3, which just meets the national military standard for uniformity of phosphor screen used in image intensifiers.

4.4.2. Uniformity at different voltages

Assuming that the current of phosphor screen is fixed at 1.37 μA , while the voltage of phosphor screen is changed in increments of 200 V from 5000 V to 6000 V. The measurement results have been shown in Table 6.

Table 6. Data of uniformity and voltage of phosphor screens

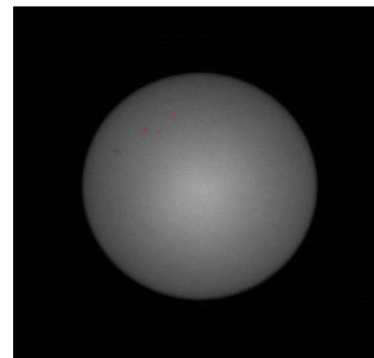
Order	Voltage of phosphor screen (V)	Uniformity
1	5000	1.64
2	5200	1.66
3	5400	1.68
4	5600	1.72
5	5800	1.77
6	6000	1.81

From Table 6, it can be seen that the luminance uniformity of phosphor screen shows little variation as the voltage increases within a certain range. Interestingly, the values of uniformity are all less than 3 as well. According to

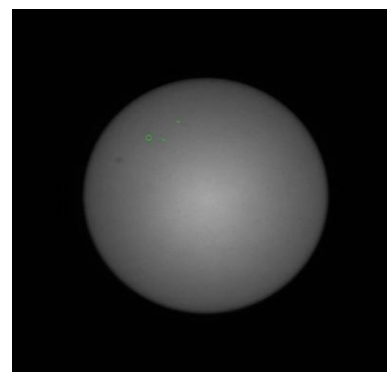
the general specifications of national military standard, the value of luminance uniformity of phosphor screens for image intensifiers should be less than 3. In other words, if the measurement value of uniformity is less than 3, this phosphor screen is considered qualified. It is very satisfying that the above discussion fully demonstrates this point.

4.5. Detection of defects of phosphor screen

To achieve optimal uniformity of the incident electron beam, the uniform planar electron source must be preheated and thereby the effect of electron beam on the defect detection of phosphor screen. After the uniform planar electron source has been preheated, the voltage of phosphor screen is fixed at 6000 V and the current of phosphor screen is set at 1.37 μA . The incident electrons are multiplied by MCP to strike the phosphor screen, resulting in the illumination of phosphor screen. At this very moment, the high-resolution camera is turned on, and focusing is conducted by a microscope to obtain the clearest image of phosphor screen, after which image acquisition can begin. The experiment involved continuous measurement over a span of 10 days, with five groups measured every day and each group consisting of 30 samples. In these experiments, manual visual inspection has been conducted simultaneously with automatic detection by algorithm. The measurement results have been categorized into the following three cases, as shown in Figs. 13, 14, and 15.



(a)



(b)

Fig. 13. Consistent results between manual inspection and automatic algorithm detection. (a) results of manual inspection; (b) results of automatic detection by algorithm

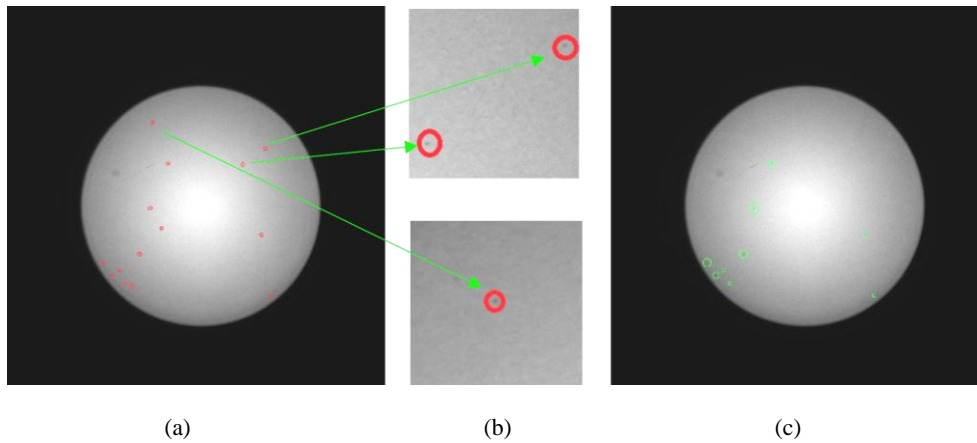


Fig. 14. Numbers of manual inspection are larger than those from automatic algorithm detection.
 (a) results of manual inspection; (b) diagram of local area; (c) results of automatic detection by algorithm (colour online)

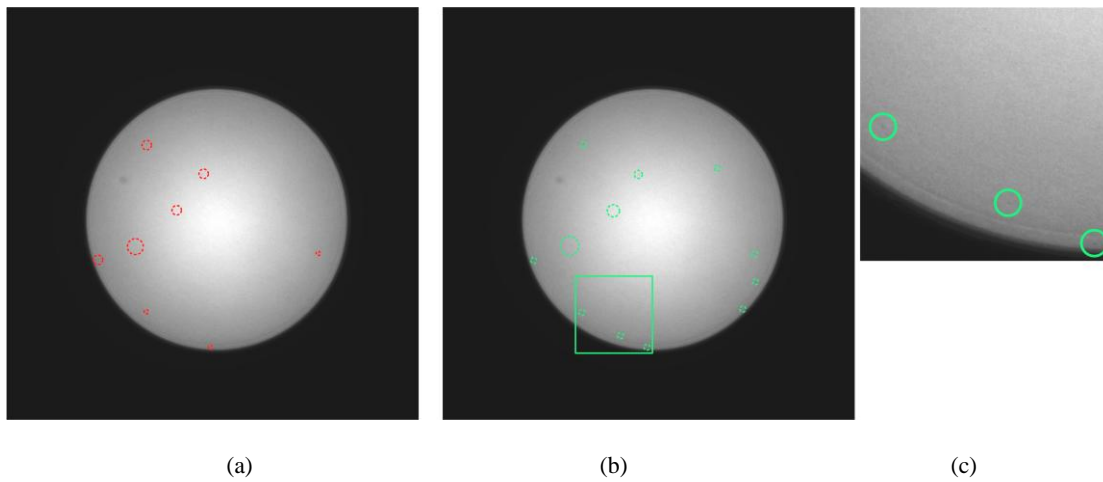


Fig. 15. Numbers of manual inspection are lower than those from automatic detection by algorithm.
 (a) results of manual inspection; (b) results of automatic detection by algorithm; (c) diagram of local area (colour online)

Concerning two cases illustrated in Figs. 14 and 15, we have made separate adjustments to corresponding algorithm. Concretely, when numbers of manual visual inspection are larger than those by algorithm detection, the threshold for image segmentation is set between the grayscale values of target pixels and background pixels, and is more closer to the values of the target pixels. This will cause some target pixels to be classified as background. Therefore, by adjusting the threshold for image binarization related to connected domains, we increased the number of target pixels, thereby increasing the number of detected defects. When numbers of manual visual inspection are lower than those by algorithm detection, since defects detected automatically by the algorithm are too small for the human eye to recognize and could be disregarded. Hence, by adjusting the threshold for connected domain area, we set this threshold to 90%, thereby eliminating defects that are too small to be identified by human eyes. Whereupon, the measurement experiment has been conducted using 10 groups of phosphor screen samples and each group consisting of 30 samples. Corresponding measurement results are shown in Table 7.

Table 7. Detected results by human eyes and algorithm

Detect tool	Defects	No defects
Human eye	216	84
Algorithm	216	84

Table 7 shows that among 300 samples of phosphor screens, the results of automatic algorithm detection is in good agreement with those of manual visual inspection. Then, using the formula (10), we have selected randomly 30 samples and calculated the accuracy a of automatic algorithm detection.

$$a = \left(1 - \sum_{i=1}^k \frac{A_i - H_i}{H_i} \right) \times 100\% \quad (10)$$

where A_i is the number of defects identified by algorithm, and H_i is the number of defects inspected by human eye,

respectively. In the end, the accuracy of automatic detection for defect using this algorithm is approximately 93.45%.

4.6. Repeatability error and detection efficiency of measurement system

The evaluation of both repeatability error and detection efficiency is crucial for ensuring the accuracy and reliability of measurement system. With reference to the automatic measurement system of phosphor screen performance for image intensifiers, we have measured the repeatability error and detection efficiency and further validated the accuracy and reliability of this rapid automatic measurement system.

4.6.1. Measurement of repeatability error

The measurement conditions are determined that the voltage of phosphor screen is 6000 V, and the current of

phosphor screen is 1.37 μ A. As for the samples, 10 group of measurement samples are taken, with each group consisting of 30 samples. Subsequently, the repeatability error measurement of luminous efficiency and uniformity for these samples has been implemented 10 times. Tables 8 and 9 show the measurement results of the repeatability error for 10 randomly selected samples.

Table 8 shows that the maximum value of repeatability error for luminous efficiency detection is 3.703%, and the average repeatability error is 3.036%. As can be seen from Table 9, it is clear that the maximum value of uniformity detection is 0.540%, the minimum value is 0.258%, and the average value is 0.369%, respectively. According to the measurement requirements, the repeatability error of luminous efficiency should be within $\pm 6\%$, these experimental data has demonstrated good repeatability of automatic measurement system of phosphor screen performance.

Table 8. Measurement result of repeatability error of luminous efficiency

Sequence	Sample 1	Sample 2	Sample 3	Sample 4	Sample 5	Sample 6	Sample 7	Sample 8	Sample 9	Sample 10
1	4.877	4.714	4.54	4.928	4.772	4.501	4.986	4.375	4.828	4.918
2	5.109	4.893	4.669	5.21	5.015	4.815	5.173	4.813	5.033	5.156
3	4.999	4.869	4.561	4.94	4.828	4.585	5.014	4.381	4.858	4.955
4	4.925	4.822	4.596	5.014	4.844	4.545	5.049	4.406	4.865	4.964
5	5.041	4.797	4.556	4.976	4.789	4.525	5.072	4.449	4.904	4.967
6	5.084	5.005	4.848	5.137	4.971	4.837	5.184	4.677	5.015	5.134
7	4.9	4.849	4.565	5.039	4.791	4.66	5.069	4.412	4.848	5.004
8	4.684	4.481	4.322	4.74	4.58	4.437	4.792	4.284	4.587	4.695
9	4.963	4.901	4.659	4.954	4.866	4.687	5	4.442	4.902	4.987
10	4.739	4.67	4.499	4.673	4.647	4.392	4.751	4.305	4.674	4.733
Repeatability error	2.824%	3.061%	2.929%	3.26%	2.72%	3.257%	2.83%	3.703%	2.807%	2.97%

Table 9. Measurement result of repeatability error of uniformity

Sequence	Sample 1	Sample 2	Sample 3	Sample 4	Sample 5	Sample 6	Sample 7	Sample 8	Sample 9	Sample 10
1	1.63	1.58	1.68	1.73	1.60	1.62	1.74	1.55	1.76	1.74
2	1.63	1.59	1.69	1.73	1.60	1.63	1.75	1.55	1.76	1.74
3	1.63	1.59	1.69	1.73	1.60	1.63	1.75	1.56	1.76	1.75
4	1.63	1.59	1.69	1.74	1.61	1.63	1.75	1.57	1.77	1.75
5	1.64	1.59	1.69	1.74	1.61	1.63	1.75	1.57	1.77	1.75
6	1.63	1.58	1.68	1.74	1.60	1.62	1.74	1.56	1.76	1.75
7	1.64	1.58	1.68	1.74	1.60	1.62	1.74	1.55	1.77	1.75
8	1.63	1.57	1.68	1.73	1.59	1.61	1.74	1.55	1.77	1.74
9	1.63	1.57	1.68	1.73	1.60	1.61	1.75	1.55	1.77	1.74
10	1.63	1.58	1.69	1.74	1.60	1.61	1.75	1.56	1.77	1.74
Repeatability error	0.258%	0.499%	0.313%	0.304%	0.355%	0.540%	0.296%	0.529%	0.292%	0.302%

4.6.2. Measurement of detection efficiency

In practical production, improving the detection efficiency of phosphor screen performance can effectively reduce production and operational costs, thereby enhancing the company's competitiveness and profitability. We have selected 300 samples of phosphor screen with diameter of 18 mm for measurement experiments. Assuming that the voltage of phosphor screen is 6000 V and the current of phosphor screen is 1.37 μ A, the average time required to inspect each phosphor screen have been obtained, by using both manual visual inspection and automatic detection methods. Specifically, the average time for manual inspection of a single phosphor screen is 52.6s, whereas the average time required for the automatic detection system to inspect a single phosphor screen is only 18.2s. Apparently, our automatic measurement system of phosphor screen performance for image intensifiers can indeed achieve fully rapid and automatic measurement of performance for a group of 30 phosphor screens with diameter of 18 mm.

5. Conclusions

To achieve rapid and automatic evaluation of phosphor screen performance for image intensifiers, we have taken some effective strategies to develop the automatic measurement system pertaining to the phosphor screen performance. Firstly, a system control logic tailored to the vacuum controller has been designed to achieve two functions. One is to achieve automatic adjustment and maintenance of vacuum level required for measurement; the other is to achieve rapid and automatic replacement of phosphor screen samples. Secondly, automatic operation of servo control system is already implemented via the precise control over the speed and direction of servo motor. Thirdly, we have designed a large-area (diameter of 50 mm) uniform planar electron source to ensure that the diameter of multiplied electron beam does completely match the diameter of phosphor screen. Lastly, combining with the developed software, our measurement system can achieve rapid and automatic batch measurement of performance of phosphor screens at 30 stations.

More importantly, the luminance, luminous efficiency, uniformity, and defect of 300 samples of phosphor screen with diameter of 18 mm which is widely used in image intensifiers have been measured. In particular, the average repeatability error of luminous efficiency and uniformity of phosphor screens are 3.036% and 0.369%, respectively. Besides, the average measurement time of a single phosphor screen is only 18.2s, and the accuracy of defect detection reaches 93.45%. Experimental results have demonstrated that rapid and automatic performance evaluation of multi-station batch for phosphor screens can be achieved. This will provide a strong evaluation tool for improving the performance of phosphor screens.

Acknowledgements

All authors thank Zhiyun Pan for his useful discussions.

References

- [1] I. P. Csorba, Image Tubes, Howard W. Sams & Co., Inc., Indianapolis (1986).
- [2] M. Purohit, A. Chakraborty, A. Lumar, B. K. Kaushik, IEEE Sens. J. **21**(6), 8530 (2021).
- [3] Y. K. Gruzhevich, M. M. Panichev, A. R. Khusnetdinov, J. Opt. Technol. **88**(3), 146 (2021).
- [4] J. H. Tan, Y. S. Song, J. R. Zhou, W. Q. Yang, X. F. Jiang, J. Liu, C. Y. Zhang, X. J. Zhou, Y. G. Xia, S. L. Liu, Chin. Phys. B **33**(8), 086102 (2024).
- [5] C. Michail, P. Liaparinis, N. Kalyvas, I. Kandarakis, G. Fountos, I. Valais, Crystals **14**, 169 (2024).
- [6] S. Varalakshmi, A. Lakshmanan, J. Lumin. **251**, 119114 (2022).
- [7] A. Shultzman, O. Segal, Y. Kurman, C. Roques-Carnes, I. Kaminer, Adv. Optical Mater. **11**(8), 2202318 (2023).
- [8] S. L. David, C. M. Michail, M. Roussou, E. Nirgianaki, A. E. Toutountzis, I. G. Valais, G. Fountos, P. F. Liaparinis, I. Kandarakis, G. Panayiotakis, IEEE Trans. Nucl. Sci. **57**(3), 951 (2010).
- [9] V. V. Postupaev, Nucl. Instrum. Meth. A **923**, 147 (2019).
- [10] D. Kim, S. Moon, W. Hwang, D. Y. Kim, Opt. Express **30**(9), 14677 (2022).
- [11] P. Scajev, A. Mekys, J. Instrum. **18**(5), P05026 (2023).
- [12] T. N. Su, F. G. Liu, R. S. Zhu, B. H. Liu, S. Cheng, M. Ji, J. Xiao, H. Zhao, L. S. Zhang, L. Chang, H. Q. Yang, J. Optoelectron. Adv. M. **26**(1-2), 28 (2024).
- [13] Y. M. Fang, Y. S. Gou, M. R. Zhang, J. F. Wang, J. S. Tian, Nucl. Instrum. Meth. A **987**, 164799 (2021).
- [14] K. Chrzanowski, B. Stafiej, Metrol. Meas. Syst. **31**(2), 339 (2024).
- [15] L. Z. Wang, Y. S. Qian, M. H. Sun, X. Y. Kong, Acta Photonica Sinica, **51**(3), 0304003 (2022).
- [16] Y. Yang, Y. S. Gou, P. H. Feng, B. Wang, B. Y. Liu, J. S. Tian, X. Wang, H. B. Liu, Nucl. Instrum. Meth. A **1056**, 168621 (2023).
- [17] L. Z. Wang, S. Tan, Y. S. Qian, S. C. Zhu, Appl. Optics **60**(23), 6888 (2021).
- [18] L. Z. Wang, Y. S. Qian, S. C. Zhu, Opt. Quantum Electron. **53**(7), 375 (2021).
- [19] L. Z. Wang, T. Cao, Y. S. Qian, Opt. Eng. **61**(6), 064102 (2022).
- [20] X. F. Bai, L. Yin, W. Hu, H. L. Shi, Y. P. He, Infrared Laser Eng. **42**(2), 495 (2013).
- [21] X. W. Ding, H. C. Cheng, Y. Yuan, R. Y. Zhang, S. N. Yang, Y. Yang, X. G. Dang, Infrared Techn. **46**(2), 129 (2024).